applied sciences

MDPI

Article

Design Considerations Concerning an Innovative Drive System for a Manual Wheelchair

Michał Kończak *, Mateusz Kukla * and Dominik Rybarczyk

Faculty of Mechanical Engineering, Poznan University of Technology, 60-965 Poznan, Poland; dominik.rybarczyk@put.poznan.pl

* Correspondence: michal.konczak@put.poznan.pl (M.K.); mateusz.kukla@put.poznan.pl (M.K.)

Abstract: Manual wheelchairs, which are the basic means of transport for people with disabilities, are usually characterized by an inefficient adaptation to the physical capabilities of their users. For this reason, it is advisable to search for solutions that will allow us to change the parameters of the mechanical power generated by human muscles. For this purpose, mechanical gearing known from other solutions, for example, from bicycles, can be used. The paper describes the design methodology and a number of issues related to the construction of an innovative wheelchair prototype using a chain transmission in its drive system. This solution allows for the implementation of a variable ratio between the wheels and the pushrims. Thus, it effectively allows for matching the demand for driving torque to the movement conditions and the physical capabilities of its user. The use of such a system provides the basis for increasing the efficiency of the manual propulsion process. Initial studies show that changing the gear ratio allows for different speeds of the wheelchair wheel. In the tests conducted, the root mean square of this value varied from 15.2 RPM to 35.5 RPM, which resulted in a change in power from 15.8 W to 40.1 W. Of course, the values of rotational speed and torque show a cyclically changing character, which results from the intermittent nature of generating drive by the wheelchair user. The average peak values of rotational speed were 31.4 ± 1.7 RPM, 44.3 ± 3.4 RPM and 57.9 ± 3.4 RPM, while the torque was 12.1 ± 0.5 Nm, 12.4 ± 0.4 Nm and 14.1 ± 0.6 Nm for Gears 1, 4 and 6, respectively.

Keywords: automatic gear; disability; drive system; manual wheelchair (MWC); mechatronic system; wheelchair

Citation: Kończak, M.; Kukla, M.; Rybarczyk, D. Design Considerations Concerning an Innovative Drive System for a Manual Wheelchair. *Appl. Sci.* **2024**, *14*, 6604. https://doi.org/10.3390/app14156604

Academic Editors: Marius Baranauskas and Rimantas Stukas

Received: 27 June 2024
Revised: 26 July 2024
Accepted: 27 July 2024
Published: 28 July 2024

1. Introduction

In its World Report on Disability, the World Health Organization (WHO) demonstrates that the issue of disability, in its broadest sense, affects around 1 billion children and adults, among whom the proportion of people experiencing severe functional difficulties is between 2.2% and 3.8%. As pointed out by the WHO, the negative median increase in the issue is also accelerated by the ageing population trend [1]. Thus, one can conclude that there is a great need for the research and development of devices that facilitate the daily functioning of people with disabilities.

Based on the current technology, several types of wheelchairs can be distinguished, depending on their driving force source [2]. The first and most popular group are manual wheelchairs, both with pushrim and crank systems [3]. They are characterized by a very good traction/stability ratio, simplicity of design while maintaining ergonomics, low weight and ease of transport. Due to the nature of the use, these wheelchairs are available in variants focused on active lifestyles, sports or driving over difficult terrain. A significant limitation for manual wheelchairs is overcoming infrastructure obstacles, such as stairs, kerbs, damaged pavements, unpaved surfaces or uphill climbs, as well as traveling long distances. An alternative to manual wheelchairs are electric or hybrid wheelchairs [4,5], which are a combination of a manual wheelchair with additional assistance via an electric

drive unit [6]. The advantages of these wheelchairs are that they dramatically increase the distance that can be covered without straining the upper limbs, and that they can be used by people with mobility issues involving the upper body as well [7]. Another advantage of this type of wheelchair may be the additional systems that allow it to overcome various types of architectural obstacles, such as kerbs or stairs, although these modifications are often associated with reduced performance in covering longer distances [8]. Disadvantages include the fact that due to the electric motor power system including a battery, these vehicles have a much higher weight compared to traditional wheelchairs, and reduced maneuverability, as well as control inertia due to the delay of the signal transmitted from the operator, through the control module, to the actuator [9,10]. A significant disadvantage of electric wheelchairs is also that they are difficult to transport in cars [11]. Paradoxically, the electric drive system, which is intended to facilitate use by replacing muscle power, results in a decrease in physical activity for people with disabilities, which may contribute to exacerbated health issues [12]. A development direction worth noting as an alternative to classical solutions is the power assist device [13,14]. These systems serve as an adaptive module for manual wheelchairs, mounted directly onto the wheelchair frame. The user controls the speed of the drive wheel via a controller, which can function as either an auxiliary or primary drive. This solution significantly reduces the number of push strokes, thereby substantially decreasing the strain on the upper limb muscles [15]. The device's weight, ranging from 6 to 8 kg, also represents a reasonable compromise given the benefits gained. Unfortunately, such devices are still new to the market and have a relatively high price. Given the advantages, disadvantages and limitations of current wheelchair solutions, and the increasing needs of wheelchair users, it makes sense to conduct research aimed at developing manual drive systems. Their most important features include lightweight, ability to fold, enabling an increase in distance travelled, making it easier to navigate uneven and unpaved terrain as well as facilitating the overcoming of architectural obstacles. At the same time, such solutions must provide a high degree of maneuverability and an easily operable system of gear changes with a simultaneous reduction in physical effort, which would directly translate into an improved condition of the user's musculoskeletal system.

Therefore, the aim of the research was to develop and construct a prototype of a wheelchair equipped with an innovative drive system that allows for changing the ratio between wheels and pushrims. An additional objective concerned verifying the prototype's operation by performing preliminary tests. They were focused on measuring the wheel rotational speed and pushrim drive torque for different values of the gear ratios.

2. Materials and Methods

2.1. Kinematic Scheme

To address the problem described, the research team decided to create a design of a manual, pushrim-propelled wheelchair with the ability to change the gear ratio (between pushrim and wheel): in both automatic and semi-automatic modes. Meeting such an assumption requires the separation of the pushrim and wheel functions, which are permanently connected in classic wheelchairs. To this end, the solution being developed is based on the patent application P.434936 (Patent Office of the Republic of Poland, 2023), which describes a pushrim ratio assembly for a manual wheelchair, and on the patent application P.443054 (Patent Office of the Republic of Poland, 2023), which refers to the wheelchair's drive wheel hub for multi-gear drive units. The kinematic system of the developed system is shown as a diagram in Figure 1. The system's most important element is the Shimano Acera CS-HG400 cassette (Shimano Inc., Sakai, Japan) enabling eight ratios including the derailleur. This is a standardized mechanism used in bicycles. For this reason, it works in a specific arrangement, because bicycles have a drive system with the chain on the right side, looking towards the direction of travel. A wheelchair has a different spatial arrangement of the driven wheels than a bicycle, so it was impossible to mirror the drive system for the right wheel relative to the wheelchair seat axis (shown on the right in the diagram), because the Shimano Acera derailleur is not able to work properly in a mirrored position [16–18].

Instead, it was decided to add a gear transmission to the right drive system, which allowed us to change the rotation direction of the chain located between the drive chain wheel and the derailleur hub. This solution also required moving the Shimano derailleur system towards the front of the wheelchair. This enabled maintaining fully identical gear ratios in the entire chain for both the wheelchair's left and right wheels, as well as a more favorable weight distribution, improving the wheelchair's stability. Table 1 presents a list of specific parameters that characterize the developed solution.

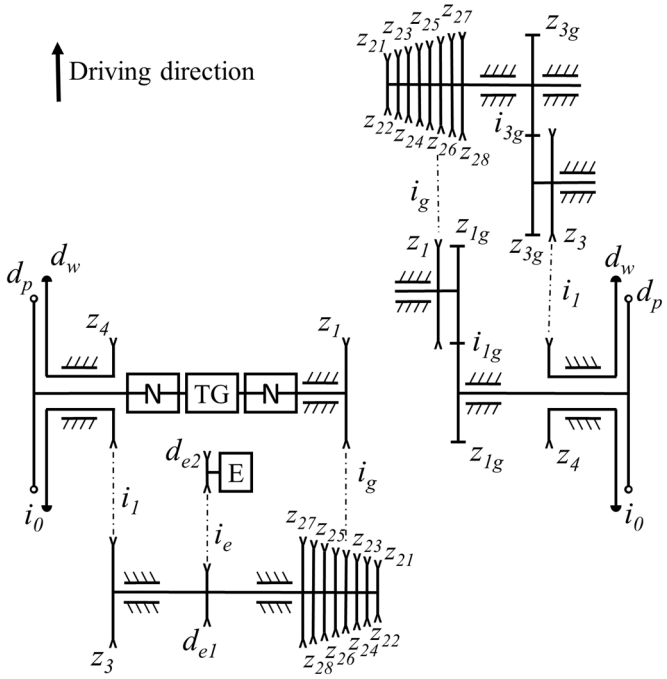

Figure 1. Kinematic diagram of the drive system of a wheelchair with a chain transmission.

Table 1. Parameters of the designed drive system.

Name	Designation	Value
Diameter of a wheel	d_w	609.6 mm
Diameter of a pushrim	d_p	520 mm
Number of sprocket teeth at the input from the wheel hub	z_1	23 teeth
Number of teeth of Shimano cassette sprockets	$z_{21}; z_{22}; z_{23}; z_{24}; z_{25}; z_{26}; z_{27}; z_{28}$	11, 13, 15, 18, 22, 27, 33, 40 teeth
Number of teeth on the countershaft sprocket	z_3	20 teeth
Number of sprocket teeth at the exit from the wheel hub	z_4	25 teeth
The number of gear teeth changing the direction of chain movement for the right wheel gear	z_{1g}	90 teeth
The number of gear teeth changing the direction of chain movement for the right wheel gear	z_{3g}	80 teeth
Torque gauge	TG	-
Encoder	E	-
Encoder pulley diameter at input	d_{e1}	54 mm
Output encoder pulley diameter	d_{e2}	24 mm

As a result, it is possible to distinguish the system's gear ratios determined by Equations (1) to (6):

$$i_0 = d_w/d_p = 609.6\ /520, \tag{1}$$

$$i_1 = z_4/z_3 = 23/20, \tag{2}$$

$$i_g = z_{21\to28}/z_1 = 0.44; 0.52; 0.60; 0.72; 0.88; 1.08; 1.32; 1.60, \tag{3}$$

$$i_{1g} = z_{1g}/z_{1g} = 90/9, \quad (4)$$

$$i_{3g} = z_{3g}/z_{3g} = 85/85, \quad (5)$$

$$i_e = d_{e2}/d_{e1} = 24/54. \quad (6)$$

The total instantaneous ratio for the left side of the i_{c1} system and the right side of the i_{c2} system is the product of the gear ratios in each stage of the mechanism included in the drive system. The ratio i_{1g} and i_{3g} for both pairs of gears changing the movement directions of the gear chain for the right gear is 1, therefore the equation for the total gear ratio (7) is as follows:

$$i_{cl} = i_{cr} = i_c, \quad (7)$$

where i_{cl} is the total gear ratio of the left wheel and i_{cr} is the total gear ratio of the right wheel.

Therefore, the system's total maximum gear ratio for each side is given as a dependency (8):

$$i_{cmax} = i_0 \cdot i_1 \cdot i_{gmax} = \frac{609.6}{520} \cdot \frac{23}{20} \cdot 1.60 = 2.157. \quad (8)$$

In turn, the system's minimum gear ratio for each side is described by Equation (9):

$$i_{cmin} = i_0 \cdot i_1 \cdot i_{gmin} = \frac{609.6}{520} \cdot \frac{23}{20} \cdot 0.44 = 0.593. \quad (9)$$

Based on the calculations, both the left and right sides of the drive system are able to implement the same ratio pairs, and based on the research it was assumed that there is bilateral symmetry in the context of the user's muscle strength [19,20]. Their range depends on the Shimano Acera derailleur setting.

2.2. Design Considerations Based on a 3D Model

A 3D model of the developed wheelchair's hub design based on the patent application P.434936 (Patent Office of the Republic of Poland, 2023) is shown in Figure 2. A ball bearing (3) and a needle bearing (4) are fitted between the upper (1) and lower (2) housings, which have been secured against displacement by means of a housing flange. The needle bearing (4) is supported by a hollow outer shaft (5), the center of which features a needle roller thrust bearing (6). The second support point of the outer shaft (4) is the sprocket wheel hub (7), which is secured against displacement by a stopper ring (8). The sprocket (7) is seated on the outer race of the ball bearing (9) supported by a stopper ring (10). Inside the outer shaft (5) is a hollow inner shaft (11), which is supported on the inner races of the needle roller bearing (6) and the ball bearing (9). On the gearbox side, the inner shaft (10) is secured with a sliding sleeve (12), bearing nut (13) and bearing washer (14). The outer shaft (5) is fitted with the wheelchair's wheel hub (15), which is secured against displacement by a stopper ring (16). The pushrim hub (17) is fitted onto to the inner shaft (11) by a keyway connection (18), on the needle roller bearing (6) side. The pushrim hub (17) is supported by a lock nut (19) screwed into the thread of the inner shaft (11). The solution is attached to the wheelchair frame by the frame clamp (20) from below and by dedicated holes in the top frame (1) from above. The design discussed differs in terms of the length of the sprocket wheel hub (7) and the inner shaft (11) in the left and right wheels, which is due to the method of connection to the gearbox and torque gauge.

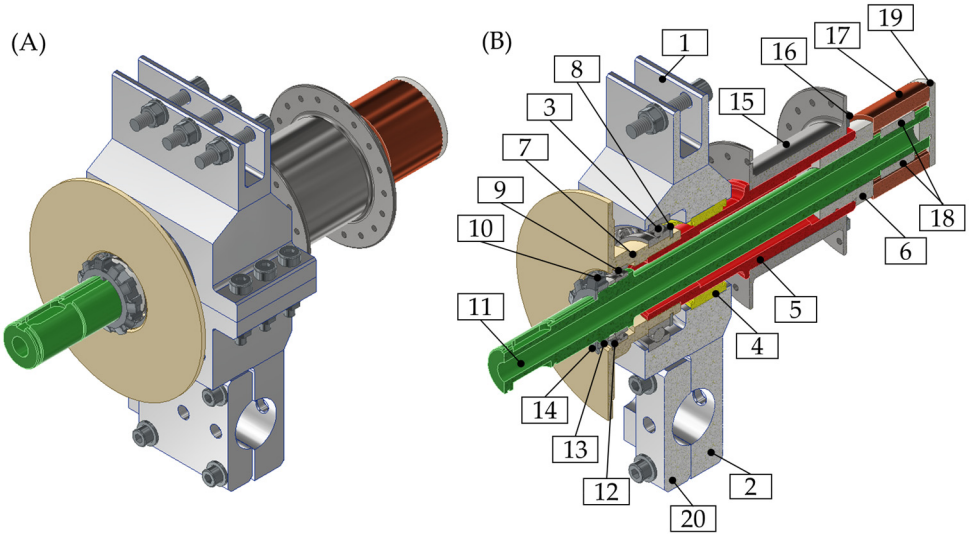

Figure 2. View of the 3D model of the developed wheelchair hub structure for the drive system on the left side of the wheelchair; (**A**) hub in isometric view, (**B**) half of the hub in isometric view.

The next step in the design process was to develop the method of fitting the created drive system to the wheelchair's frame. The Vermeiren V300 wheelchair (Vermeiren Poland, Trzebnica, Poland) was chosen as the basis for this task, thereby enabling the determination of the frame's geometry. The final stage of the system's construction required the modeling of its remaining components. Once the non-standardized parts were designed and standardized components selected, their geometry was mapped in the CAD environment. This enabled the development of an overall assembly of the prototype drive system solution for the left and right wheels.

It is worth mentioning that the right wheel assembly had to be modified due to the lack of a torque gauge and the bicycle derailleur's inability to work in a mirror image. This is an important issue and a significant technical problem to solve in the future, as such a solution is disadvantageous. The prototype after complete assembly is shown in Figure 3.

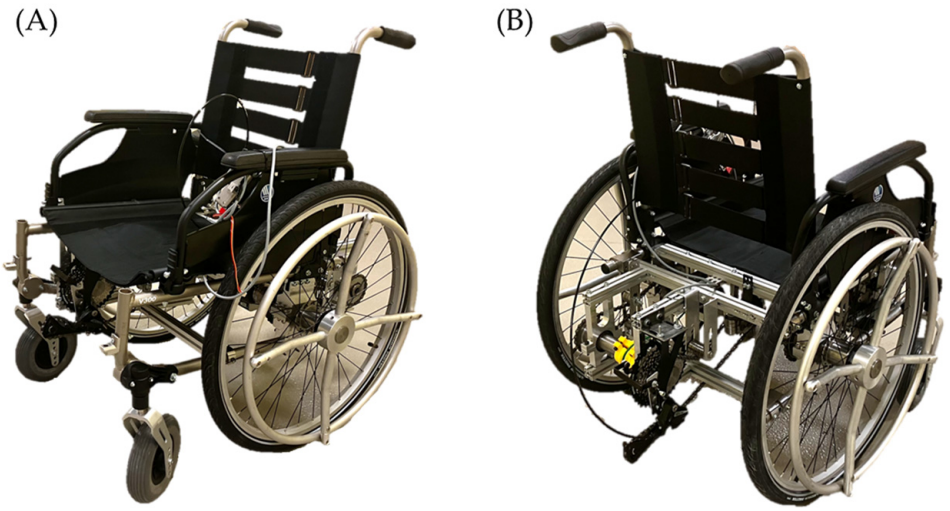

Figure 3. *Cont.*

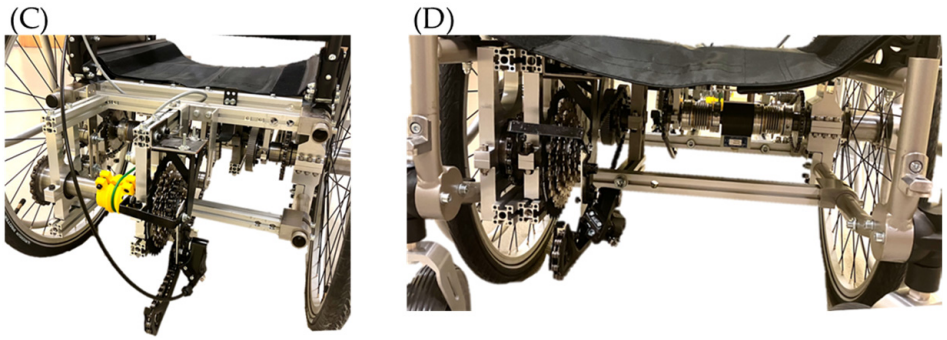

Figure 3. Prototype view: (**A**) isometric view from the left side, (**B**) isometric view from the right side, (**C**) assembly for the left wheel drive system—rear view, (**D**) assembly for the right wheel drive system—front view. The footrests have been removed to increase visibility of the drive system.

The current prototype version (proof of concept) has a mass of 43 kg, and this would need to be reduced in a commercial system. Such weight results from the installation of the drive system in a ready-made, commercially available wheelchair. Designing the solution from scratch based on an FEA strength analysis carried out for structures made of lightweight alloys or composites would probably reduce its mass [21,22]. As part of optimizing the mechanism, it is also worth paying attention to the development of micro air vehicles, which also utilize modified chain drives as presented in several studies [23,24]. Moreover, minimizing the weight of the wheelchair will directly translate into a reduction in the value of forces acting on the wheelchair–human system, reducing, for example, friction forces [25,26].

2.3. Electronic Control System

Once the prototype was built, work began on designing the automatic gear ratio change system. The developed system operates using a DC servomotor; a T22/10NM torque meter (Hottinger Brüel & Kjaer GmbH, Darmstadt, Germany) working in the current standard; an HY38-500 push–pull type incremental encoder (Termipol, Lubliniec, Poland) working at 5 VDC; as well as communication with the user via a touch HMI display (Nextion, Shenzhen, China). The first step in building the electronic system controlling the derailleur was to develop an electrical diagram. The system's central point is the STM32L432 microcontroller (STMicroelectronics, Geneva, Switzerland). The power supply is provided by two adjustable pulse converters set to two voltage ranges: 12 V for the torque meter and the microcontroller module, and 6 V for the servo. A pack of 4 lithium-ion cells, i.e., Li-Ion Samsung INR18650-25R 2500 mAh cell (Samsung SDI Co., Ltd., Yongin, Republic of Korea) was selected as the voltage source. They can be easily replaced in the event of discharge. They can also be expanded to a larger capacity if a longer operating time is needed. The control system's block diagram is presented in Figure 4.

The assembly of the ratio shifting mechanism is shown in Figure 5. The servomotor (21) is connected to the derailleur tensioner lever (22) by means of a handle (23). The derailleur tensioner lever (22) is mounted on a mandrel (24) connected to the servo mount (25), which is screwed to its body.

The control module can operate in two modes: semi-automatic, controlled by the user using a touch panel, or automatic. In the latter operating mode, the shift occurs when the set value of the drive torque measured by a torque meter installed on the pushrim hub shaft is exceeded. The ranges of drive torque for a given gear ratio are fully editable through data entered into the controller. This will enable optimal range adjustment in the future based on the results collected based on tests carried out on the test group, taking into account muscle tension tests in order to verify the reduction in their load [27,28]. The changes in the center of gravity [29] and the range of movements of individual upper limb parts [30], which, as the authors prove, has a significant impact on the driving torque generation by the user's musculoskeletal system, must also be taken into account.

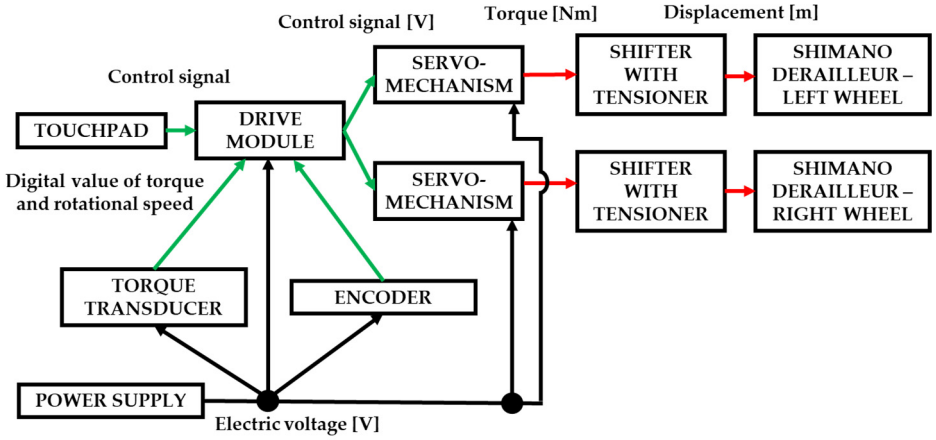

Figure 4. Block system diagram of the control.

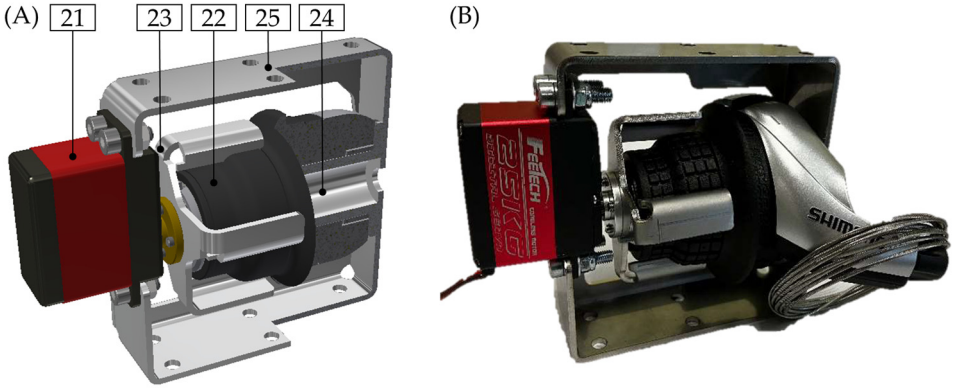

Figure 5. Assembling the gear changing mechanism (**A**) quarter view, (**B**) view of the constructed mechanism.

2.4. Measurement Methodology

Verification of the effectiveness and proper operation of the created structure required testing. A wheelchair dynamometer developed according to the patent application P.444414 (Patent Office of the Republic of Poland, 2023) was used to carry out the testing. It is a test bench that allows the simulation of various scenarios of manual wheelchair propulsion, enabling the simultaneous measurement of a number of biomechanical parameters. A detailed description of the dynamometer is beyond the scope of this elaboration—it can be found, for example, in [31]. First, the tested wheelchair was placed on the dynamometer and immobilized, as shown in Figure 6. User-driven scenarios were then performed for the entire 8-speed derailleur range. To obtain comparable results, the participant propelled the wheelchair to the rhythm of a metronome set at 40 BPM, which corresponds to a wheelchair velocity of about 4.3 km/h (1.9 m/s). The wheel rotation speed was measured with an incremental encoder (as shown on Figure 1) [32]. The torque supplied to the drive system was determined based on a torque meter measurement. The tests were not carried out on a wider population because their primary purpose was to demonstrate the principles and correct operation of the designed device. Work aimed at qualitative and quantitative assessment of the developed wheelchair's effectiveness, using a larger number of volunteers, is currently in progress. This study was accepted by the Bioethical Commission at Karol Marcinkowski Medical University in Poznan, Poland (Resolution No. 513/21 of 24 June 2021, under the guidance of MD M. Krawczyński for the research team led by M. Kukla).

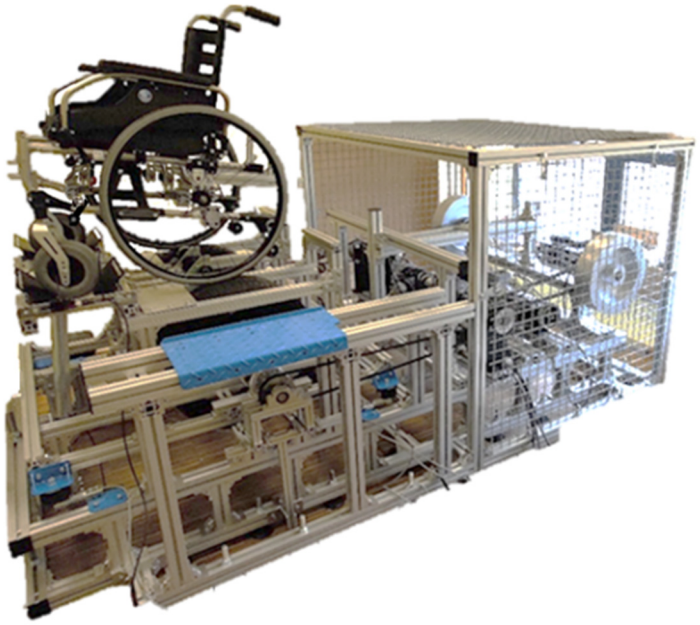

Figure 6. A prototype wheelchair mounted on a dynamometer.

3. Results and Discussion

Figure 7 shows the dependency between the wheelchair velocity and drive torque relative to a selection of three ratios representing Gears 1, 4 and 6, for which the overall ratios are 0.592, 0.97 and 1.455, respectively. This illustrated the drive system's operation consecutively in different modes: reduction mode, an approximately one-to-one gear ratio and multiplication.

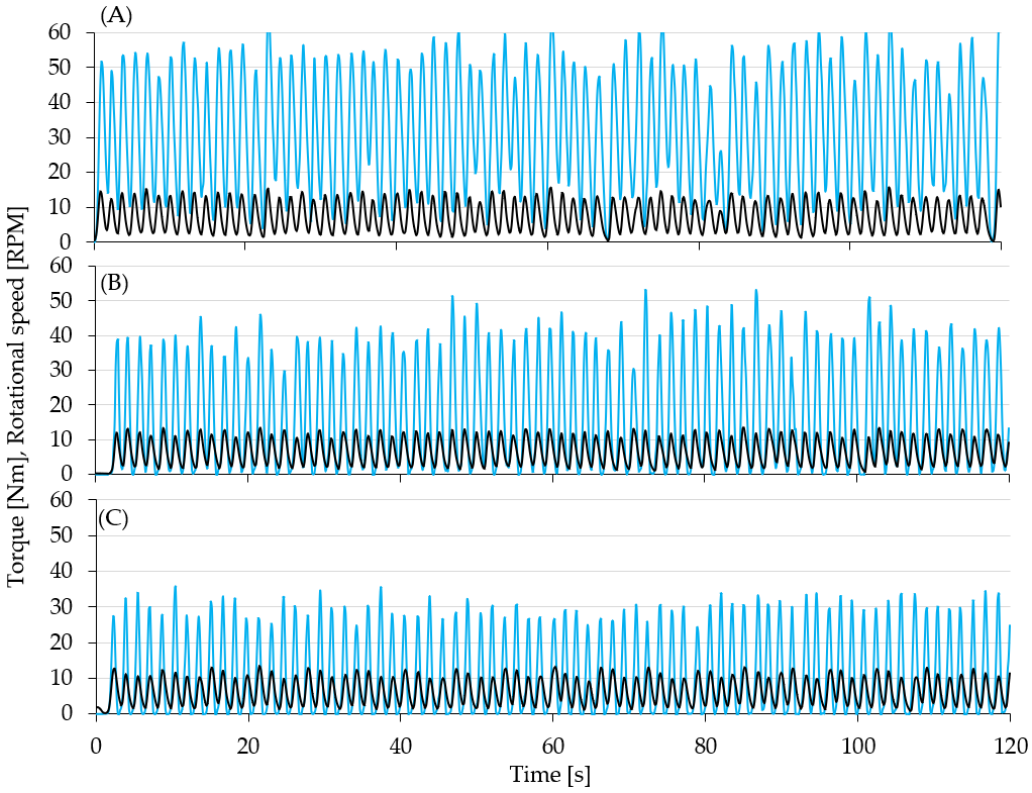

Figure 7. Graph of the change in rotational speed and torque as a function of time, taking into account the gear ratio. (**A**) Gear 1, (**B**) Gear 4, (**C**) Gear 6.

An analysis of the presented graph makes it possible to observe the cyclical nature of individual propulsion phases. It stems from the way the wheelchair is propelled. The user propels the pushrims with their hands at a certain rotation angle, thereby creating a driving torque. In the next phase of the propulsion cycle, moving the upper limbs to the initial position is necessary. This is dictated by the biomechanics of the human body. In the graph, this moment can be observed as a reduction in torque and velocity. In some cases, the cessation of propelling causes the torque value to drop to zero. At the same time, the cessation of propulsion generation does not cause the velocity to drop to zero, as the inertia accumulated in the drive system results in a gradual loss of speed. This can be observed in Figure 7a. This results from the fact that the successive propulsion phases could occur sufficiently quickly to prevent the occurring drag forces (e.g., friction) from acting long enough to brake the rotating wheels.

Based on the results, it was found that a shift in the gears to higher ratios translates directly into an increase in the wheelchair's wheel speed. The individual incremental values for both wheel speed and drive torque correspond to pushrims' propulsion. The peak values, on the other hand, occur at the final phase of the upper limb movement, just before the user's hand releases the pushrim. The recorded wheel speed corresponds to the calculated theoretical values. The peak drive torques for the selected ratios ranged from 11.3 to 15.7 Nm. In turn, the recorded peak values for rotational speed were in the range from 29 RPM to 66.9 RPM.

For the purpose of comparing the values for individual ratios, the root mean square (RMS) of the recorded waveform was determined due to its cyclical nature [33]. The calculated values for individual physical quantities are presented in Table 2.

Table 2. RMS values of measured physical quantities.

Gear Number [27,28]	Torque [Nm]	Rotational Speed [RPM]	Power [W]
1	7.1	15.2	15.8
3	7.3	22.7	24.9
6	8.5	35.5	40.1

Analysis of the graphs presented in Figure 7 and the values in Table 2 allows us to observe that the root mean square values of the driving torque are not constant. The in-crease in the torque value for Gear 1 compared to Gear 4 is only about 3%, but for Gear 6 it is already 16%—which constitutes a significant value. This change is probably due to two factors. As the wheel rotation speed increases, the resistance to movement also in-creases due to friction but, above all, the inertia of the moving elements (both in the drive system of the wheelchair and the dynamometer itself). Moreover, in the experiment the controlled factor was the frequency of driving phases (by using a metronome), not the value of speed or driving torque. Therefore, the user could apply different amounts of force when generating the drive in the following propulsion phases. This is the influence of the human factor, which cannot be avoided in this type of research.

The recorded data were then further processed to calculate the mechanical power in the drive system. As shown in Figure 8, an increase in the ratio results in an increase in power, leading to the conclusion that the designed drive mechanism is not a constant power system. This is mainly due to the increase in rotational speed values. The RMS value of the mechanical power was 15.8 W for Gear 1, 24.9 W for Gear 4 and 40.1 W for Gear 6—however, the peak values were much larger, as can be seen in the graph in Figure 8.

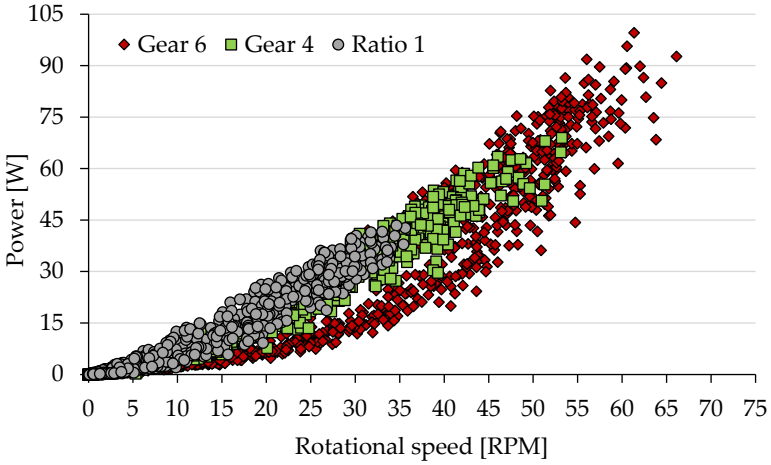

Figure 8. Drive power graph for Gears 1, 4 and 6.

The obtained results can be correlated with the study [34], which presented a comparison of propulsion force generation for a conventional wheelchair and a handcycle. Based on the obtained results, it can be concluded that the created drive system prototype allows for propelling the wheelchair with the same propulsion force over a similar speed range as in the case of the handcycle. This represents a significant improvement in the efficiency of wheelchair propulsion and a reduction in the load on the upper limb and shoulder girdle muscles, considering that only about 50% of the user's generated muscle force is transformed into propulsion force [35,36]. The results of the tested prototype for Gear 4 with a ratio of 0.97 did not significantly deviate from the conventional solution, which in turn proves the correctness of the selected gear ratios relative to the initial assumptions. Qualitative verification of the changes in the user's upper limb and whole-body load will be determined by surface electromyography (EMG) measurements [37,38] and metabolic parameter measurements [39–41].

4. Conclusions

The work carried out involved the designing and manufacture of a prototype of a manual wheelchair with an innovative drive system equipped with an electronic shifting system operating in manual or automatic mode. The prototype's testing phase confirmed the design's correct operation. The ratio range selection allows the drive to operate in the reduction and multiplication range, but also with a ratio of 0.97, which practically corresponds to the classic solution, where the pushrim is permanently connected to the wheel-chair's wheel rim (neutral ratio). This means that the designed wheelchair may make it easier to climb hills, kerbs or unpaved terrain, as well as to cover longer distances at higher speeds. Plans for the future involve carrying out a specific study on a test group consisting of people with physical disabilities. The obtained data will enable the effective adjustment of the torque range for the automatic ratio shift mode. In order to qualitatively verify the changes in upper limb load, further studies will be conducted using EMG and measurements of metabolic parameters.

Potential directions of future development may include FEA strength analysis carried out for structures made of lightweight alloys or composites, while maintaining system rigidity, which can translate into a significant extension of the equipment's service life. This will also enable a reduction in the wheelchair's own weight, which will also reduce rolling resistance and therefore the demand for drive torque. The strive towards minimizing the wheelchair's own weight is a welcome development, as it affects its performance, including transport.

There are also limitations related to the presented study and prototype. It should be emphasized, however, that the prototype presented in this paper has not been subjected to an optimization process. A very important factor in the aspect of a wheelchair is

its own weight. The pursuit of mass minimization is justified because it affects a large number of parameters related to movement, as it reduces the value of the forces acting in the wheelchair–human system, which effectively limits, for example, the friction forces. Additionally, the arrangement according to the presented design deprives the wheelchair of the ability to fold. This was necessitated, among other things, by the need to install a torque meter and the correct installation of the chain transmission using the derailleur.

5. Patents

Kukla, M. et. al. Patent application of the automatic chain transmission mechanism for a traction-driven wheelchair (original title in Polish: Mechanizm automatycznej przekładni łańcuchowej dla wózka inwalidzkiego z napędem ciągowym). Patent Office of the Republic of Poland, P.447665, 2024.

Kukla, M. et. al. Patent application of the modification kit for converting a classic manual derailleur controlled by a twist grip into a derailleur controlled by electric signals. (original title in Polish: Zespół modyfikacyjny do konwersji klasycznej przerzutki manualnej sterowanej manetką obrotową w przerzutkę sterowaną za pomocą sygnałów elektrycznych). Patent Office of the Republic of Poland, P. 447680, 2024.

Author Contributions: Conceptualization, M.K. (Michał Kończak) and M.K. (Mateusz Kukla); methodology, M.K. (Michał Kończak) and M.K. (Mateusz Kukla); software, D.R.; validation, M.K. (Michał Kończak), M.K. (Mateusz Kukla), and D.R.; formal analysis, M.K. (Michał Kończak) and M.K. (Mateusz Kukla); investigation, M.K. (Michał Kończak) and M.K. (Mateusz Kukla); resources, M.K. (Michał Kończak) and M.K. (Mateusz Kukla); data curation, M.K. (Michał Kończak) and M.K. (Mateusz Kukla); writing—original draft preparation, M.K. (Michał Kończak); writing—review and editing, M.K. (Mateusz Kukla) and D.R.; visualization, M.K. (Michał Kończak) and M.K. (Mateusz Kukla); supervision, M.K. (Mateusz Kukla); project administration, M.K. (Mateusz Kukla); funding acquisition, M.K. (Mateusz Kukla). All authors have read and agreed to the published version of the manuscript.

Funding: This research is a part of the project: "Innovative Drive Systems for Wheelchairs—Design, Prototype, Research", number: "Rzeczy są dla ludzi/0004/2020" financed by National Centre for Research and Development, https://www.gov.pl/web/ncbr (accessed on 3 October 2021).

Institutional Review Board Statement: The research results presented in this article are part of a large project: "Innovative Drive Systems for Wheelchairs: Design, Prototype, Research", number: "Rzeczy są dla ludzi/0004/2020". All research planned as part of this project was approved by the bioethics committee. The research received (a positive opinion from the bioethics committee at the K. Marcinkowski Medical University in Poznań—Committee Resolution No. 513/21 of 24 June 2021).

Informed Consent Statement: Informed consent was obtained from all subjects involved in this study.

Data Availability Statement: The data that support the findings of this study are available from the corresponding author upon reasonable request.

Conflicts of Interest: The authors declare no conflicts of interest.

References

1. Hartley, S.; Jessup, N.; Madden, R.; Officer, A.; Posarac, S.; Shakespeare, T. The way forward: Recommendations. In *World Report on Disability*; World Health Organization: Geneva, Switzerland, 2011; ISBN 978-92-4068-800-1.
2. Sydor, M. *Selecting and Using a Wheelchair (orginal Polish title: Wybór i eksploatacja wózka inwalidzkiego)*; Publishing House of the Agricultural University of A. Cieszkowski in Poznań: Poznan, Poland, 2003; pp. 20–26. ISBN 83-7160-315-0.
3. Fiok, K. *Parametric Optimization of an Innovative Manual Wheelchair (original title in Polish: Optymalizacja parametryczna innowacyjnego wózka inwalidzkiego z napędem ręcznym)*; Warsaw University of Technology: Warsaw, Poland, 2014; pp. 15–26.
4. Yang, L.; Guo, N.; Sakamoto, R.; Kato, N.; Yano, K. Electric Wheelchair Hybrid Operating System Coordinated with Working Range of a Robotic Arm. *J. Robot. Control.* **2022**, *3*, 679–689. [CrossRef]
5. Ravindu, H.M.; Priyanayana, K.S.; Pathirana, C.D.; Jayasekara, B. Hybrid Navigation Decision Control Mechanism for Intelligent Wheel-Chair. *Inst. Electr. Electron. Eng. Access* **2023**, *11*, 118558–118576. [CrossRef]
6. Sydor, M.; Zabłocki, M.; Torzyński, D. Functional translation of user needs into wheelchair design. In *Scientific Papers of the Poznań University of Technology. Organization and Management*; Poznań University of Technology Publishing House: Poznan, Poland, 2017; pp. 214–216. [CrossRef]

7. de Souza, L.H.; Frank, O.A. Problematic clinical features of powered wheelchair users with severely disabling multiple sclerosis. *Disabil. Rehabil.* **2015**, *37*, 990–996. [CrossRef] [PubMed]
8. Ning, M.; Yu, K.; Zhang, C.; Wu, Z.; Wang, Y. Wheelchair design with variable posture adjustment and obstacle-overcoming ability. *J. Braz. Soc. Mech. Sci. Eng.* **2021**, *43*, 197. [CrossRef]
9. Levy, C.E.; Buman, M.P.; Chow, J.W.; Tillman, M.D.; Fournier, K.A.; Giacobbi, P., Jr. Use of power assist wheels results in increased distance traveled compared with conventional manual wheeling. *Am. J. Phys. Med. Rehabil.* **2010**, *89*, 625–634. [CrossRef] [PubMed]
10. Kloosterman, M.G.; Snoek, G.J.; van der Woude, L.H.; Buurke, J.H.; Rietman, J.S. A systematic review on the pros and cons of using a pushrim-activated power-assisted wheelchair. *Clin. Rehabil.* **2012**, *27*, 299–313. [CrossRef] [PubMed]
11. Giacobbi, P., Jr.; Levy, C.E.; Dietrich, F.D.; Winkler, S.H.; Tillman, M.D.; Chow, J.W. Wheelchair users' perceptions of and experiences with power assist wheels. *Am. J. Phys. Med. Rehabil.* **2010**, *89*, 225–234. [CrossRef] [PubMed]
12. Andrew, O.F.; de Souza, L.H. Clinical features of children and adults with a muscular dystrophy using powered indoor/outdoor wheelchairs: Disease features, comorbidities and complications of disability. *Disabil. Rehabil.* **2017**, *40*, 1007–1013. [CrossRef]
13. Jang, D.J.; Kim, Y.C.; Hong, E.P.; Kim, G.S. Development of Power-Assist Device for a Manual Wheelchair Using Cycloidal Reducer. *Appl. Sci.* **2023**, *13*, 954. [CrossRef]
14. Khalili, M.; Eugenio, A.; Wood, A.; Van der Loos, M.; Bennett Mortenson, W.; Borisoff, J.F. Perceptions of power-assist devices: Interviews with manual wheelchair users. *Disabil. Rehabilitation. Assist. Technol.* **2021**, *18*, 1–11. [CrossRef]
15. Dhaliwal, M.; Janssen, S.; Kuik, K.; Giesbrecht, E.M. *Choosing a Power Assist Device*; Rady Faculty of Health Sciences University of Manitoba: Winnipeg, MB, Canada, 2021. [CrossRef]
16. Weng, F.T.; Jenq, S.M. Designing of Rear Derailleur Mechanism on Bicycle. *J. Comput. Theor. Nanosci.* **2013**, *19*, 2336–2339. [CrossRef]
17. Casteel, E.A.; Archibald, M. A Study on the Efficiency of Bicycle Hub Gears. In Proceeding of the ASME 2013 International Mechanical Engineering Congress and Exposition, San Diego, CA, USA, 15–21 November 2013. [CrossRef]
18. Levarda, E. Bicycle transmissions. *IOP Conf. Ser. Mater. Sci. Eng.* **2018**, *444*, 052013. [CrossRef]
19. Kukla, M.; Maliga, W. Symmetry Analysis of Manual Wheelchair Propulsion Using Motion Capture Techniques. *Symmetry* **2022**, *14*, 1164. [CrossRef]
20. Figas, G.; Hadamus, A.; Błażkiewicz, M.; Kujawa, J. Symmetry of the Neck Muscles' Activity in the Electromyography Signal during Basic Motion Patterns. *Sensors* **2023**, *23*, 4170. [CrossRef] [PubMed]
21. Kalyanasundaram, S.; Lowe, A.; Watters, A. Finite element analysis and optimization of composite wheelchair wheels. *Compos. Struct.* **2006**, *75*, 393–399. [CrossRef]
22. Keangin, P.; Chawengwanicha, P.; Wimala, N.; Nakbanpotkul, T. Structural analysis of three-dimensional finite element model to design multifunction wheelchair for patients. *IOP Conf. Ser. Mater. Sci. Eng.* **2021**, *1137*, 12054. [CrossRef]
23. Chen, L.; Cheng, C.; Zhou, C.; Zhang, Y.; Wu, J. Flapping rotary wing: A novel low-Reynolds number layout merging bionic features into micro rotors. *Prog. Aerosp. Sci.* **2024**, *146*, 100984. [CrossRef]
24. Phan, H.V.; Park, H.C. Insect-inspired, tailless, hover-capable flapping-wing robots: Recent progress, challenges, and future directions. *Prog. Aerosp. Sci.* **2019**, *111*, 100573. [CrossRef]
25. Sprigle, S.; Huang, M.; Lin, J.T. Inertial and frictional influences of instrumented wheelchair wheels. *J. Rehabil. Assist. Technol. Eng.* **2016**, *3*, 1–5. [CrossRef]
26. Sprigle, S.; Huang, M. Impact of Mass and Weight Distribution on Manual Wheelchair Propulsion Torque. *Assist. Technol. Off. J. RESNA* **2015**, *27*, 226–235. [CrossRef]
27. Raez, M.B.I.; Sajjad Hussain, M.; Mohd-Yasin, F. Techniques of EMG signal analysis: Detection, processing, classification and applications. *Biol. Proced. Online* **2006**, *8*, 11–35. [CrossRef] [PubMed]
28. Hof, A.L. EMG and muscle force: An introduction. *Hum. Mov. Sci.* **1984**, *3*, 119–153. [CrossRef]
29. Wieczorek, B.; Kukla, M.; Warguła, Ł. The symmetric nature of the position distribution of the human body center of gravity during propelling manual wheelchairs with innovative propulsion systems. *Symmetry* **2021**, *13*, 154. [CrossRef]
30. Wieczorek, B.; Kukla, M.; Warguła, Ł. Describing a Set of Points with Elliptical Areas: Mathematical Description and Verification on Operational Tests of Technical Devices. *Appl. Sci.* **2022**, *12*, 445. [CrossRef]
31. Kończak, M.; Kukla, M.; Warguła, Ł.; Rybarczyk, D.; Wieczorek, B. Considerations for the Design of a Wheelchair Dynamometer concerning a Dedicated Braking System. *Appl. Sci.* **2023**, *13*, 7447. [CrossRef]
32. Briz, F.; Cancelas, J.A.; Diez, A. Speed measurement using rotary encoders for high performance AC drives. In Proceedings of the Proceedings of IECON'94-20th Annual Conference of IEEE Industrial Electronics, Bologna, Italy, 5–9 September 1994; Volume 1. [CrossRef]
33. Colominas, J.; Pallas-Areny, R. A new method for measuring RMS values. *Inst. Electr. Electron. Eng. Xplore* **1986**, *74*, 1468–1469. [CrossRef]
34. Arnet, U.; van Drongelen, S.; Veeger, D.; van der Woude, L.H.V. Force Application During Handcycling and Handrim Wheelchair Propulsion: An Initial Comparison. *J. Appl. Biomech.* **2013**, *29*, 687–695. [CrossRef]
35. Boninger, M.; Cooper, R.; Robertson, R.; Shimada, S. Three-dimensional pushrim forces during two speeds of wheelchair propulsion. *Am. J. Phys. Med. Rehabil.* **1997**, *76*, 420–426. [CrossRef] [PubMed]

36. Jenkins, A. Analysis of a Lever-Driven Wheelchair Prototype and the Correlation Between. *IFAC Proc. Vol.* **2014**, *47*, 9895–9900. [CrossRef]
37. Mills, K.R. The basics of electromyography. *Br. Med. J.* **2005**, *76*, 32–35. [CrossRef] [PubMed]
38. Elamvazuthi, I.; Duy, N.H.X.; Zulfiqar, A.; Su, S.W.; Khan, A.; Parasuraman, S. Electromyography (EMG) based Classification of Neuromuscular Disorders using Multi-Layer Perceptron. *Procedia Comput. Sci.* **2015**, *76*, 223–228. [CrossRef]
39. Pierce, R. Spirometry: An essential clinical measurement. *Aust. Fam. Physician* **2005**, *34*, 535–539. [PubMed]
40. wen Sewa, D.; Ong, T.H. Pulmonary Function Test: Spirometry. *Proc. Singap. Healthc.* **2014**, *23*, 57–64. [CrossRef]
41. Paraskeva, M.; Borg, B.M.; Naughton, M.T. Spirometry. *Aust. Fam. Physician* **2011**, *40*, 216–219. [PubMed]